

# Electron attachment by chloro and bromomethanes

James K. Olthoff,<sup>a)</sup> John H. Moore, and John A. Tossell

Department of Chemistry, University of Maryland, College Park, Maryland 20742

(Received 15 November 1985; accepted 21 March 1986)

Electron transmission spectra and mass spectra of negative ions from dissociative electron attachment have been obtained for the series  $\text{CCl}_4$ ,  $\text{CBrCl}_3$ ,  $\text{CBr}_2\text{Cl}_2$ , and  $\text{CBr}_4$ . Systematic changes are observed in the attachment energies of the  $t_2$  unoccupied orbitals in the end members and their split components in the mixed compounds.  $\text{Cl}^-$  and  $\text{Br}^-$  ion-production maxima are observed to correspond to attachment energies measured by ETS. Multiple scattering- $X\alpha$  continuum calculations give elastic-electron-scattering cross sections for  $\text{CCl}_4$  and  $\text{CBr}_4$  which are consistent with experiment in the low energy region, but fail to reproduce the maximum in total cross section observed at higher energy. Calculated and experimental valence orbital I.P.'s and UV excitation energies for  $\text{CCl}_4$  and  $\text{CBr}_4$  are shown to be consistent with our electron transmission results.

## INTRODUCTION

Electron capture and subsequent dissociation of halo-gen-substituted methanes has received considerable attention recently. This is in part due to the significance of such processes to atmospheric chemistry<sup>1</sup> and to the application of haloalkanes as gaseous dielectrics.<sup>2</sup> The energetics of low-energy electron capture by molecules can be studied by electron transmission spectroscopy (ETS). The technique is well established in the study of substituted alkenes where the spectra display well-defined features due to shape resonances associated with electron capture into specific molecular orbitals.<sup>3</sup> The analysis of such spectra employs the "composite molecule" or "molecules-in-molecules" approach.<sup>4</sup> By this method each feature in the spectrum is assigned to an orbital associated with a molecular fragment, such as a substituent or a portion of the unsaturated backbone. This approach is not appropriate for substituted alkanes where the spectra of the parent hydrocarbons are featureless, and those of the haloalkanes show only weak and rather broad features. Perhaps the difficulties with interpretation and the rather uninteresting appearance of the spectra account for the paucity of ETS data on the haloalkanes.

The electron transmission spectra of some chloromethanes and chlorofluoromethanes have been reported by Burrow *et al.*<sup>5</sup> Their assignment of the observed anion states, although plausible, was based upon virtual-orbital energies derived from small-basis-set-SCF calculations for the neutral molecules. This approach can at best yield relative electron affinities, and in fact, a discrepancy between calculation and experiment of about 3 eV was postulated and a number of unobserved states were predicted.<sup>5</sup> Of course electron transmission spectroscopy involves a scattering process, so any such bound-state approach is suspect.

Unlike electron transmission data, there is a large amount of data on the dissociation of halomethanes.<sup>6-12</sup> Most of these studies concentrate upon the chlorinated or fluorinated methanes because of their environmental importance. However, little effort has been made to correlate dis-

sociative attachment data with electron transmission spectra, although such a connection is expected and is observed for unsaturated halocarbons previously studied.<sup>13</sup>

In the present work we have investigated both electron transmission and dissociative attachment in the family of bromochloromethanes ( $\text{CCl}_4$ ,  $\text{CBrCl}_3$ ,  $\text{CBr}_2\text{Cl}_2$ ,  $\text{CBr}_4$ ). To aid in making orbital assignments, as well as in understanding the scattering process, we present appropriate bound-state and continuum quantum calculations.<sup>14-16</sup> We also make quantitative comparison of our results with UV absorption and photoemission, as well as other ETS data,<sup>17</sup> in an attempt to substantiate our assignments. Our data overlap that of Burrow *et al.*<sup>5</sup> in the case of  $\text{CCl}_4$  where our calculations as well as other data from the literature confirm their assignment of the first ETS feature to the  $^2T_2$  anion, thus implying that the  $^3A_1$  ground-state anion is stable.

## EXPERIMENT

The apparatus used for the study of low-energy electron capture and dissociative attachment is an electron transmission spectrometer to which a time-of-flight mass spectrometer (TOFMS) has been appended. The electron transmission spectrometer has been described in detail elsewhere<sup>13</sup> so only a brief explanation will be given here. A detailed summary of the mass spectrometer follows.

Electron transmission spectroscopy is a technique for measuring the energy of a temporary negative ion formed by electron capture into an unoccupied orbital of a molecule. The experiment involves the measurement of the transparency of a gas to an electron beam as a function of energy. The transparency depends in an inverse fashion upon the electron-scattering cross section. Temporary negative ion formation occurs with a large cross section only over a narrow energy range. The negative ion promptly decays by giving up the trapped electron or by dissociative attachment. The formation and decay process appears as a sharp fluctuation in the electron-scattering cross section. This process, as well as the corresponding feature in the transmission vs electron energy spectrum, is referred to as a "resonance."

The electron spectrometer<sup>18</sup> consists of an electron source followed by an electron monochromator, a gas cell,

<sup>a)</sup> Present address: Pharmacology Department, The Johns Hopkins School of Medicine, Baltimore, Maryland.



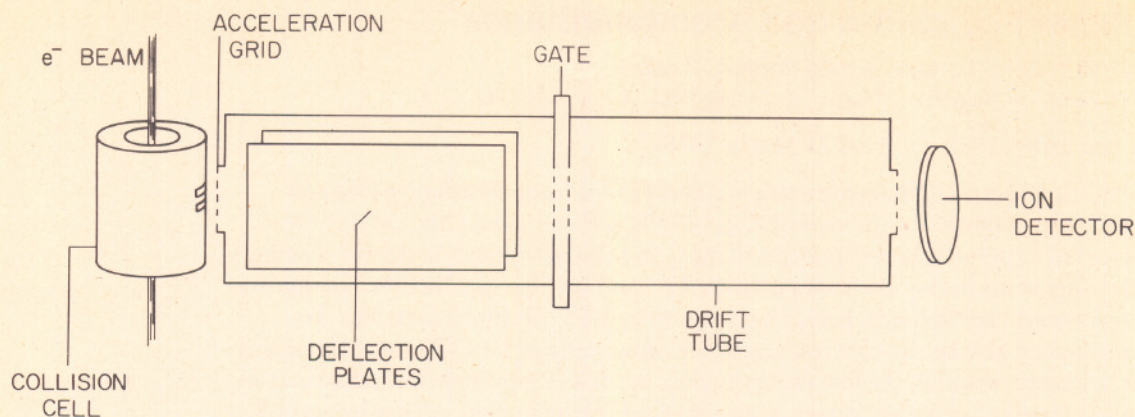


FIG. 1. Schematic diagram of the time-of-flight mass spectrometer. The electron spectrometer collision cell is immersed in a magnetic field of 70 G.

and an electron collector. The electron beam is aligned by a homogeneous magnetic field ( $B = 70$  G) generated by a pair of Helmholtz coils mounted outside the vacuum system. The spectrometer is baked daily to  $350^\circ\text{C}$  to ensure stable operation after exposure to molecular compounds. In practice the first derivative of the transmitted current as a function of energy is recorded since the derivative is sensitive to the abrupt change in transmitted current associated with a resonance.<sup>19</sup> The energy associated with a resonance is known as an "attachment energy" (A.E.) and, with respect to the derivative spectrum, is taken to be the point vertically midway between the minimum and the maximum which characterize the resonance. The electron energy scale is calibrated with reference to features in the  $\text{N}_2$  spectrum near 2 eV.<sup>20</sup> For the present purposes, an attachment energy may be identified with the negative of the corresponding vertical electron affinity (E.A.).<sup>21</sup>

Dissociation of a temporary negative anion into a stable negative ion and a stable neutral fragment may occur if the nuclei have sufficient time to move before the electron is reemitted and if sufficient energy is available to break the necessary bonds. The mass and kinetic energy of the resultant stable ion can be determined by measuring its velocity following acceleration through a known potential difference. In the present experiment the mass resolution of the TOFMS is better than 1 amu for ions with mass less than 150 amu, and the kinetic energy may be determined to within 0.1 eV.

The TOFMS is attached to the electron transmission spectrometer's gas cell, and consists of a deflection tube, followed by a gate, a drift tube, and an ion detector (Fig. 1). Ions drift out of the collision chamber and are accelerated by 20.00 eV as they enter the deflection tube. The deflection tube contains a pair of electrodes which create an electric field perpendicular to the magnetic field generated by the ETS Helmholtz coils. The Coulomb force opposes the Lorentz force, thus allowing the ions to reach the field-free region outside of the Helmholtz coils. Here the ions encounter a gate, consisting of a series of grids, at the entrance to a 40 cm drift tube. A 30 ns, 20 V pulse opens the gate. Ions which drift the length of the tube are detected by a copper-beryllium, focused mesh, electron multiplier. All of the units of the

TOFMS (with the exception of the detector) are constructed of nonmagnetic stainless steel and are baked daily to  $350^\circ\text{C}$  to ensure the same stable operation obtained from the electron transmission spectrometer.

The mass spectrometer is also used to produce a second type of spectrum. By applying a constant voltage to the TOFMS gate and drift tube, ions may arrive continuously at the detector. Then scanning the electron energy produces an ion production rate vs electron energy spectrum. The crossed electric and magnetic fields in the deflection tube act as a Wien filter which allows some mass selection. For compounds which produce only one species of ion, or for compounds which produce ions with large mass differences, an ion production rate vs electron energy spectrum for a single mass is obtained. The halogen ions,  $\text{F}^-$ ,  $\text{Cl}^-$ , and  $\text{Br}^-$ , all have sufficient mass differences to allow them to be separated by the Wien filter. This type of data has the same energy resolution as the electron transmission data.

## RESULTS

The derivative electron transmission spectra of  $\text{CCl}_4$ ,  $\text{CBrCl}_3$ ,  $\text{CBr}_2\text{Cl}_2$ , and  $\text{CBr}_4$  are presented in Fig. 2. Two low-energy features are present for  $\text{CBr}_2\text{Cl}_2$ , and one for each of the remaining compounds. The single feature in  $\text{CBrCl}_3$  does however exhibit some indication of a second overlapping resonance. The number of resonances observed for each compound can be explained by a simple model in which one anion state is associated with each carbon-halogen bond. Thus as suggested by Burrow *et al.*,<sup>5</sup>  $\text{CCl}_4$  and  $\text{CBr}_4$  (with  $T_d$  symmetry) are expected to have an anion state with  $A_1$  symmetry and a triply degenerate anion state of  $T_2$  symmetry. However, there is evidence that the ground state anions of both  $\text{CCl}_4$  and  $\text{CBr}_4$  have positive vertical electron affinities<sup>22</sup> and thus cannot be observed by electron transmission spectroscopy. Multiple-scattering  $X\alpha$  (MS- $X\alpha$ ) calculations of the electron affinities of  $\text{CCl}_4$  and  $\text{CBr}_4$ , using the bound transition state approach, give  $-0.1$  and  $+1.4$  eV, respectively, in reasonable agreement with the experimental values<sup>21</sup> of  $+0.15$  and  $+1.17$  eV obtained from studies of the spectra of donor-acceptor complexes. Thus, a single anion state of  $T_2$  symmetry is expected to be observed for both



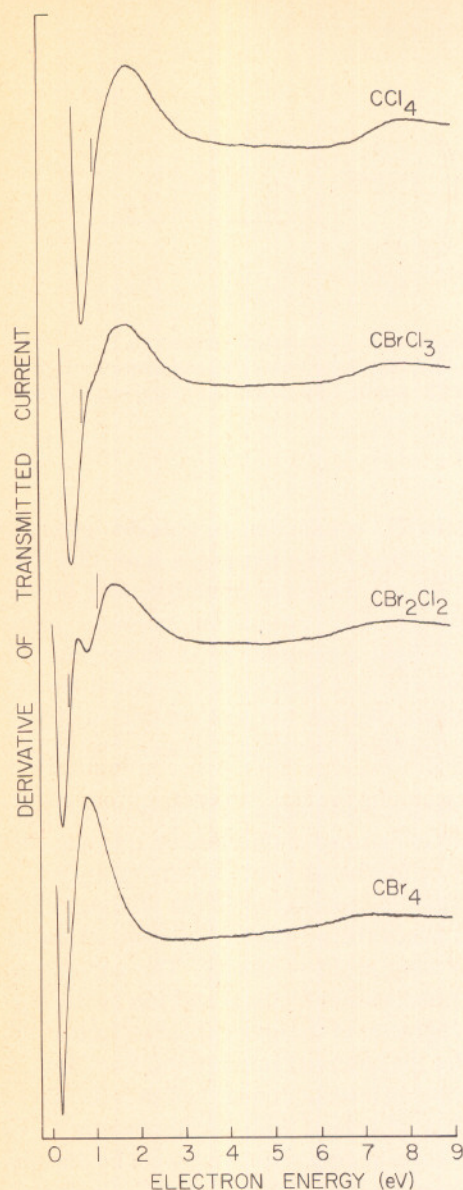


FIG. 2. Derivative electron transmission spectra of  $\text{CCl}_4$ ,  $\text{CBr}_3\text{Cl}$ ,  $\text{CBr}_2\text{Cl}_2$ , and  $\text{CBr}_4$ .

$\text{CCl}_4$  and  $\text{CBr}_4$ . For  $\text{CBrCl}_3$  ( $C_{3v}$  symmetry) the triply degenerate  $T_2$  state is split into a doubly degenerate anion state of  $E$  symmetry and a second anion of  $A_1$  symmetry. Because bromine and chlorine have very similar electron properties, the bromine substitution is expected to only slightly perturb the molecular system from the  $\text{CCl}_4$  electronic configuration in which case the splitting between the  $E$  and  $A_1$  states may be small. This would account for the unusual shape of the  $\text{CBrCl}_3$  electron transmission feature. For  $\text{CBr}_2\text{Cl}_2$  the  $E$  anion state is split into two states of  $B_1$  symmetry both of which should be observed. The second  $A_1$  state is probably considerably higher in energy and the corresponding feature in the spectrum would be very broad.

Continuum MS- $X\alpha$  calculations have been employed to obtain explicit scattering cross section for  $\text{CCl}_4$  and  $\text{CBr}_4$ . For  $\text{CBr}_4$  the experimental internuclear distance of 1.942

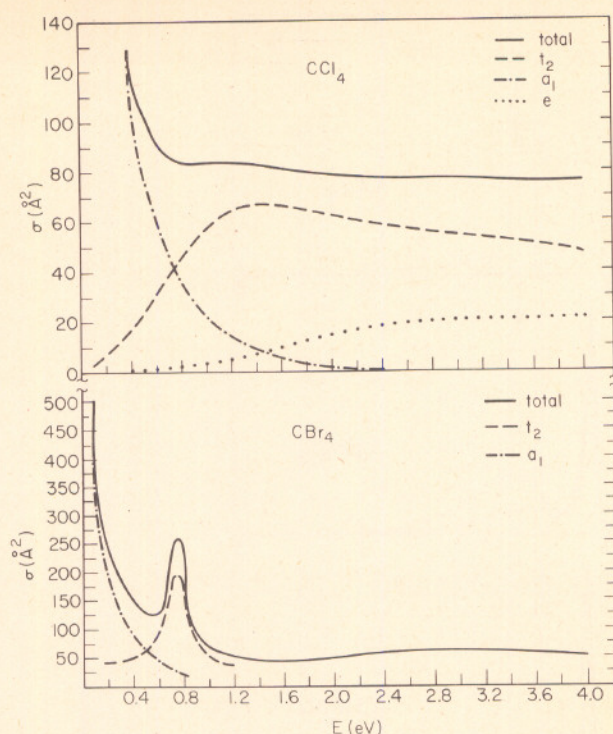


FIG. 3. Continuum MS- $X\alpha$  elastic electron scattering cross sections for  $\text{CCl}_4$  and  $\text{CBr}_4$ ; (—) total, (---)  $t_2$ , (-·-)  $a_1$ , (···)  $e$ . (Note that a factor of 2 error in the  $\text{CCl}_4$  cross section of Ref. 16 has been corrected.)

$\bar{A}$ ,<sup>23(a)</sup> standard  $\alpha$ 's,<sup>23(b)</sup> and standard sphere sizes<sup>23(c)</sup> were used (Fig. 3). The calculations support the assignments made above for  $\text{CCl}_4$  and  $\text{CBr}_4$  in the low energy region. Beyond 4 eV the calculated cross section is monotonically decreasing for  $\text{CBr}_4$ , with no indication of the second broad feature seen near 5.5 eV in the electron transmission data. For  $\text{CCl}_4$  the cross section shows a weak maximum at about 6 eV, perhaps consistent with the experimental feature at 6.5 eV. This 6.0 eV maximum arises from a competition between increasing cross sections in some channels and decreasing cross-sections in others, and does not appear to be a resonant effect. Thus, the  $\text{CCl}_4$  and  $\text{CBr}_4$  cross sections are qualitatively similar, but the  $t_2$  resonance is more distinct for  $\text{CBr}_4$ , partly due to its larger cross section and partly due to weaker competition from  $a_1$  scattering. Since the  $a_1$  resonance is calculated to lie slightly above threshold, but experiment<sup>22</sup> indicates it to be slightly below (i.e., a bound state with a barely positive E.A.), our calculations probably exaggerate the  $a_1$  contribution near threshold in  $\text{CCl}_4$ . Comparison with measured absolute cross sections<sup>17</sup> for  $\text{CCl}_4$  indeed indicates that our calculated  $t_2$  cross section has its maximum at about the right energy and has about the right magnitude but that it is too broad and the  $a_1$  contribution adding to it near threshold is too high.

The yield of  $\text{Cl}^-$  and  $\text{Br}^-$  ions as a function of electron energy is presented in Fig. 4. Above 3 eV only very small numbers of ions were detected. The  $\text{CCl}_4$  dissociation spectrum is very similar to those published previously.<sup>6,8</sup> The most notable features of the ion spectra are the threshold peaks. The cross section for dissociative attachment near



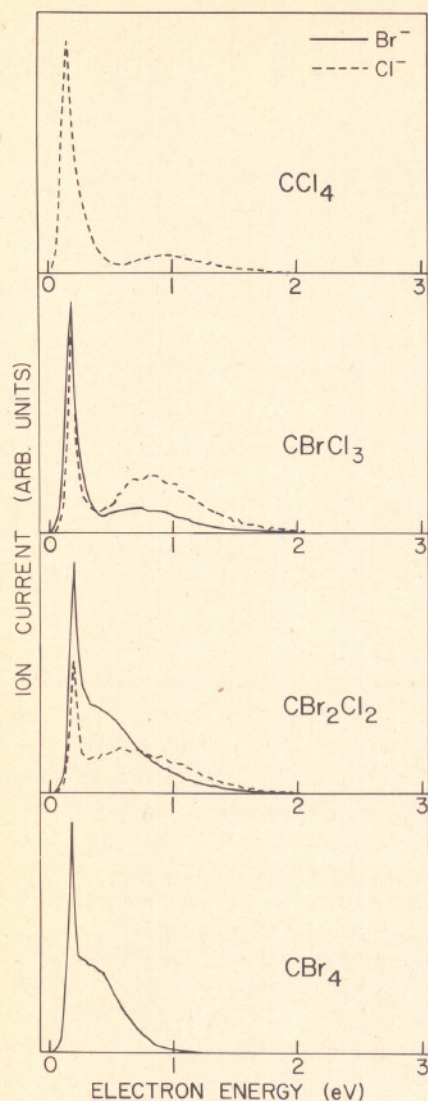


FIG. 4.  $\text{Cl}^-$  and  $\text{Br}^-$  yields as a function of electron energy for  $\text{CCl}_4$ ,  $\text{CBrCl}_3$ ,  $\text{CBr}_2\text{Cl}_2$ , and  $\text{CBr}_4$ .

threshold in these compounds is enormous as has been observed by Chutjian and co-workers<sup>24</sup> for the case of attachment to  $\text{CCl}_4$  by electrons of energy less than 50 meV and as is implied by our calculations above. These overwhelming attachment processes have a deleterious effect upon the performance of our apparatus at very low electron energies. The shape and location of the threshold peaks were found to be strongly dependent upon sample gas pressure. With increasing pressure the threshold peaks broaden and their apparent maxima move to higher energies. With decreasing pressure the threshold peaks become narrow and move toward lower energy. Apparently the residual sample background pressure outside the sample cell ( $< 5 \times 10^{-6}$  Torr) attenuates the incident current near threshold. As a result our experiments cannot be expected to characterize the shape of the cross section vs energy function at energies below 0.15 eV.

Each of the dissociation spectra also exhibit one ion peak below 1 eV. In  $\text{CBrCl}_3$  the  $\text{Cl}^-$  and  $\text{Br}^-$  ion peak loca-

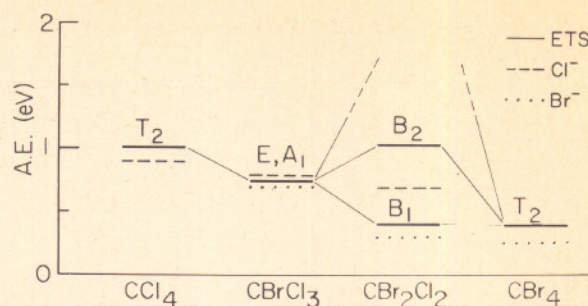


FIG. 5. Correlation diagram giving attachment energies (A.E.) for  $\text{CCl}_4$ ,  $\text{CBrCl}_3$ ,  $\text{CBr}_2\text{Cl}_2$ , and  $\text{CBr}_4$ . Suggested anion state assignments are given. Energies of maxima for  $\text{Cl}^-$  and  $\text{Br}^-$  production due to dissociative attachment are also indicated.

tions coincide, but the  $\text{Cl}^-$  production exceeds  $\text{Br}^-$  production by 3 to 1. For  $\text{CBr}_2\text{Cl}_2$  the ion peaks have different locations. Overall  $\text{Br}^-$  is the more abundant ion, but at slightly higher energies  $\text{Cl}^-$  production becomes more prominent. Time-of-flight measurements indicate that all the ions are created with less than 0.1 eV of initial kinetic energy. The attachment energies, ion peak energies, and possible anion state assignments are presented as a correlation diagram in Fig. 5.

Locations of the ion peaks near 1 eV correspond quite well to the positions of features in the electron transmission spectra. The tendency for the ion peaks to fall slightly below the resonance energies is expected since the lifetime of the resonant state and hence the probability of dissociation increases with decreasing electron energy. The correlation between electron transmission features and ion peaks suggests the bonding character of the unoccupied molecular orbitals responsible for the observed anion states. For  $\text{CBr}_2\text{Cl}_2$  the electron transmission resonance near 1 eV must be due to electron capture in a  $\sigma^*$  orbital with predominantly C-Cl character, and the lower energy resonance must be due primarily to electron capture into a  $\sigma^*$  orbital of C-Br character. Similarly, the single feature in  $\text{CCl}_4$  and  $\text{CBr}_4$  may be assigned to electron capture into orbitals with C-Cl and C-Br character, respectively. However, for  $\text{CBrCl}_3$  it is still

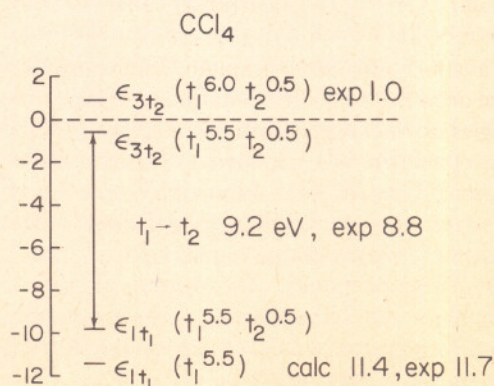


FIG. 6. Relationships between valence orbital ionization potentials, UV excitation energies, and attachment energies for  $\text{CCl}_4$  using the transition state model.



TABLE I. Ionization potentials and UV absorption energies (in eV) for  $\text{CCl}_4$  and  $\text{CBr}_4$  from MS- $X\alpha$  calculations and experiment.

	$\text{CCl}_4$		$\text{CBr}_4$	
	Calc	Exp <sup>a</sup>	Calc	Exp <sup>a</sup>
$1t_1$ I.P.	11.4	11.7	10.1	10.6
$Xnbt_2$ I.P.	12.2	12.5	10.8	11.3
$1t_1 \rightarrow \text{empty } a_1$	8.2	7.0 <sup>b</sup>	4.0	4.9 <sup>c</sup> (sh)
$1t_1 \rightarrow \text{empty } t_2$	9.2	8.8 (8.4 sh)	7.4	
$Xnbt_2 \rightarrow \text{empty } a_1$	9.0	9.2	4.6	5.5
$Xnbt_2 \rightarrow \text{empty } t_2$	10.0	9.5	8.0	

<sup>a</sup>Reference 30.<sup>b</sup>Reference 31.<sup>c</sup>Reference 32.

uncertain whether the ETS feature near 0.7 eV is a single resonance or two overlapping features. We cannot determine from the ion data if there exist two nearly degenerate orbitals (one with C-Cl character and one with C-Br character), or whether there exists only one orbital with mixed C-Cl, C-Br character.

The mechanism giving rise to the threshold peaks in the ion production spectra may be similar to that observed for dissociative attachment to HCl which has its maximum at 0.8 eV,<sup>25</sup> far below the ETS peak at 3.3 eV<sup>26</sup> which corresponds to occupation of the  $\sigma^*$  orbital. Domcke and Cederbaum<sup>27</sup> have suggested that a low-lying  $\sigma^*$  anion state coupled to the continuum will produce resonance activity near threshold. The  $^2T_2$  state in  $\text{CCl}_4$  and  $\text{CBr}_4$  may also be such a low energy  $\sigma^*$  state. Another possibility is that dissociation at low energies is caused by a resonant state created just above threshold by the bound  $A_1$  state of these compounds. It is well known that a potential well which possesses an energy level just below zero will give rise to resonant scattering of low energy electrons.<sup>24,28</sup> MS- $X\alpha$  calculations support this second possibility since they predict a large increase in scattering cross section for both  $\text{CCl}_4$  and  $\text{CBr}_4$  at very low energies due to interaction with the  $A_1$  channel. However, small errors in the calculated energies of the  $A_1$  states may significantly affect these calculated cross sections. Another interpretation<sup>29</sup> focuses more generally upon the close approach of the potential curve of the anion and that of the ground vibrational level of the neutral molecule in the Franck-Condon region.

For the end members we can, as explained previously,<sup>15</sup> relate the valence orbital I.P.'s UV excitation energies, and attachment energies, within the transition state approach as shown in Fig. 6. The MS- $X\alpha$  method gives reasonably accurate values for all three quantities. As shown in Table I, the I.P.'s and UV excitation energies of  $\text{CBr}_4$  are also obtained accurately. We can thus establish that our assignment of the ETS peaks at 1.0 eV in  $\text{CCl}_4$  and 0.4 eV in  $\text{CBr}_4$  to a  $^2T_2$  resonance state is quantitatively consistent with experimental values for the  $t_1$  orbital IP's and the  $t_1 \rightarrow t_2$  orbital excitation energies. The valence term energy for the  $a_1$  orbital ( $1t_1$  I.P. -  $1t_1 \rightarrow \text{empty } a_1$  UV excitation) is considerably more positive in  $\text{CBr}_4$  than in  $\text{CCl}_4$  (5.7 vs 4.7 eV, experimentally). This is consistent with a positive value for the E.A. for

the  $^2A_1$  ion state of  $\text{CBr}_4$  and supports our contention that the orbital lies below threshold in ETS.

## CONCLUSIONS

The electron transmission spectra of the chlorobromomethanes can be interpreted in the low-energy region in terms of occupation of the  $t_2 \sigma^*$  orbital and its split components. Cross sections for  $\text{Cl}^-$  and  $\text{Br}^-$  formation are found to be significantly energy dependent. Likewise the proportion of fragment free radicals, such as  $\text{CCl}_2\text{Br}$  and  $\text{CClBr}_2$  from  $\text{CCl}_2\text{Br}_2$ , are energy dependent. Maxima in the  $\text{Cl}^-$  and  $\text{Br}^-$  yields correspond to the attachment energies measured by ETS. Multiple scattering- $X\alpha$  calculations reproduce the valence orbital I.P.'s and excitation energies for the end members with reasonable accuracy. The low energy ETS resonance arising from the  $t_2 \sigma^*$  orbital is also described fairly well but for  $\text{CCl}_4$  the  $a_1$  contribution to the cross section is exaggerated.

## ACKNOWLEDGMENTS

This work was supported by National Science Foundation Grant No. CHE-84-17759 and by the Computer Science Center of the University of Maryland. J.H.M. was supported in part by a fellowship from the General Research Board of the University of Maryland.

<sup>1</sup>F. S. Rowland and H. J. Molina, Rev. Geophys. Space Phys. **13**, 1 (1972).<sup>2</sup>L. G. Christophorou, *Gaseous Dielectrics II* (Pergamon, New York, 1980).<sup>3</sup>K. D. Jordan and P. D. Burrow, Acc. Chem. Res. **11**, 341 (1979).<sup>4</sup>J. Wayne Rabalais, *Principles of Ultraviolet Photoelectron Spectroscopy* (Wiley, New York, 1977), pp. 286-323.<sup>5</sup>P. D. Burrow, A. Modelli, N. S. Chiu, and K. D. Jordan, J. Chem. Phys. **77**, 2699 (1982).<sup>6</sup>H.-U. Scheunemann, E. Illenberger, and H. Baumgartel, Ber. Bunsenges. Phys. Chem. **84**, 580 (1980).<sup>7</sup>W. E. Wentworth, R. George, and H. Keith, J. Chem. Phys. **51**, 1971 (1969).<sup>8</sup>D. Spence and G. J. Schulz, J. Chem. Phys. **58**, 1800 (1973).<sup>9</sup>G. J. Verhaart, W. J. Van Der Hart, and H. H. Brongersma, Chem. Phys. **34**, 161 (1978).<sup>10</sup>D. L. McCorkle, A. A. Christodoulides, L. G. Christophorou, and I. Syamrej, J. Chem. Phys. **72**, 4049 (1980).<sup>11</sup>E. Illenberger, H.-U. Scheunemann, and H. Baumgartel, Chem. Phys. **37**, 21 (1979).



- <sup>12</sup>H.-U. Scheunemann, M. Heni, E. Illenberger, and H. Baumgartel, Ber. Busenges. Phys. Chem. **86**, 321 (1982); E. Illenberger, *ibid.* **86**, 252 (1982).
- <sup>13</sup>J. K. Olthoff, J. A. Tossell, and J. H. Moore, J. Chem. Phys. **83**, 5627 (1985).
- <sup>14</sup>D. Dill and J. L. Dehmer, J. Chem. Phys. **61**, 692 (1974); J. W. Davenport, W. Ho, and J. R. Schrieffer, Phys. Rev. B **17**, 3115 (1978).
- <sup>15</sup>J. A. Tossell and J. W. Davenport, J. Chem. Phys. **80**, 813 (1984).
- <sup>16</sup>An error of a factor of 2 in previously reported cross sections [see: J. A. Tossell and J. W. Davenport, J. Chem. Phys. **83**, 4824 (1985)] has been corrected in the results reported here.
- <sup>17</sup>R. K. Jones, J. Chem. Phys. **84**, 813 (1986).
- <sup>18</sup>A. Stamatovic and G. S. Schulz, Rev. Sci. Instrum. **41**, 423 (1970); M. R. McMillan and J. H. Moore, *ibid.* **51**, 944 (1980).
- <sup>19</sup>L. Sanche and G. J. Schulz, Phys. Rev. **45**, 1672 (1972).
- <sup>20</sup>P. D. Burrow and J. A. Michejda, Chem. Phys. Lett. **42**, 223 (1976).
- <sup>21</sup>For a discussion of A.E.'s vs E.A.'s see: J. C. Giordan, M. R. McMillan, J. H. Moore, and S. W. Staley, J. Am. Chem. Soc. **102**, 4870 (1980).
- <sup>22</sup>M. Hatano and O. Ito, Bull. Chem. Soc. Jpn. **44**, 916 (1971).
- <sup>23</sup>(a) *Tables of Interatomic Distances and Configurations in Molecules and Ions*, edited by L. E. Sutton (Chemical Society, London, 1965); (b) K. Schwarz, Phys. Rev. B **5**, 2466 (1972); (c) J. G. Norman, J. Chem. Phys. **61**, 4630 (1974).
- <sup>24</sup>A. Chutjian and S. H. Alajajian, Phys. Rev. A **31**, 2885 (1985); A. Chutjian, S. H. Alajajian, J. M. Ajello, and O. J. Orient, J. Phys. B **17**, L745 (1984).
- <sup>25</sup>L. G. Christophorou, R. N. Compton, and H. W. Dickson, J. Chem. Phys. **48**, 1949 (1968); R. Abouaf and D. Teillet-Billy, J. Phys. B **10**, 2661 (1977).
- <sup>26</sup>J. A. Tossell, J. H. Moore, and J. C. Giordan, Inorg. Chem. **24**, 1100 (1985).
- <sup>27</sup>W. Domcke and L. S. Cederbaum, J. Phys. B **14**, 149 (1980).
- <sup>28</sup>L. I. Schiff, *Quantum Mechanics* (McGraw-Hill, New York, 1968).
- <sup>29</sup>D. D. Clarke and C. A. Coulson, J. Chem. Soc. A **1969**, 169.
- <sup>30</sup>J. C. Green, M. L. H. Green, P. J. Joachim, A. F. Orchard, and D. W. Turner, Philos. Trans. R. Soc. London Ser. A **268**, 111 (1970).
- <sup>31</sup>B. R. Russell, L. O. Edwards, and J. W. Raymonla, J. Am. Chem. Soc. **95**, 2129 (1973).
- <sup>32</sup>M. Ito, P. C. Huang, and E. M. Kosower, J. Chem. Soc. Faraday Trans. **57**, 1662 (1961).







